

https://dspace.org/

Lowcost instrumentation for high frequency ultrasonic guided wave laboratory research in free rock bolts

Philip Loveday; Paul Fromme

https://hdl.handle.net/10539/47420
WOS

Downloaded from a DSpace repository. https://dspace.org/

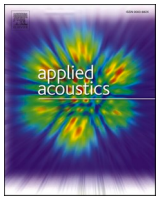
Applied Acoustics 227 (2025) 110262



Contents lists available at ScienceDirect

Applied Acoustics

journal homepage: www.elsevier.com/locate/apacoust



Low-cost instrumentation for high frequency ultrasonic guided wave laboratory research in free rock bolts

Philip W. Loveday [a,*], Paul Fromme [b]

[a] University of the Witwatersrand, Johannesburg, South Africa
[b] Department of Mechanical Engineering, University College London WC1E 7JE, UK

ARTICLE INFO

Keywords:
Low-cost instrumentation
Guided wave ultrasound measurements
Inspection of rock bolts
USB oscilloscope versus bench-top instruments

ABSTRACT

Guided wave ultrasound offers the ability to inspect slender structures from a single transducer location. However, the propagation of guided waves is more complex than the propagation of bulk waves used in conventional ultrasonic testing, and the experimental equipment required is more sophisticated. Typical equipment is expensive and may limit research and industrial application. This paper investigates what can be achieved by using low-cost instrumentation for laboratory measurements. The application is the measurement of guided waves in rock bolts (cylindrical rods) at relatively high frequencies (5 MHz). The dispersive wave propagation requires the use of narrowband excitation signals. The use of a bench-top waveform generator and oscilloscope is compared to the use of a compact and low-cost USB oscilloscope, which includes an arbitrary waveform generator. The introduction of a pre-amplifier mitigated the poorer noise performance of the USB oscilloscope, and comparable results were obtained from the two setups. It is demonstrated that waves propagated 9 m in a free rock bolt, with 10 dB/m attenuation, could be detected and analyzed with a measurement setup costing approximately USD 1110.

1. Introduction

In conventional nondestructive ultrasonic testing bulk compressional or shear waves, which propagate in an infinite solid medium are used and a structure may be scanned using an ultrasonic transducer to inspect for corrosion or cracks [1]. As an alternative, guided wave ultrasound propagates in structures with boundaries that guide the propagation of the ultrasonic energy. These guided waves may propagate with relatively low attenuation and therefore offer the potential for inspecting a large volume of a structure from a single transducer location [2–4]. This makes it possible to monitor structures in real time as only a few permanently installed sensors are required [5]. Another advantage of guided wave ultrasound is that inaccessible parts of a structure, such as embedded rock bolts or insulated pipes, may be inspected [6,7]. Numerous applications of guided wave ultrasound are currently being researched to exploit these advantages. Typical geometries that support guided wave propagation include pipes, rods, beams, rails, plates, and shells [8]. Guided wave ultrasound has mostly seen industrial application for the inspection and monitoring of pipelines, especially in the oil and gas industry, and commercial equipment for pipes is readily available [1,9]. Other applications being developed include rock bolts [10], rail track [11,12], and aerospace applications [13–15].

While the advantages of guided wave ultrasound make it attractive for the monitoring of large structures, there are also some challenges that have limited the adoption of the technology. These include the more complex wave propagation of guided wave ultrasound compared to bulk wave ultrasound [8]. There are typically many different possible modes of propagation in a waveguide, and these modes propagate with dispersion because energy at different frequencies propagates at different velocities [8]. Measurement of ultrasonic guided waves requires different equipment compared to conventional ultrasonic testing to deal with this added complexity. The signals received from guided wave ultrasound measurements may therefore be complex and in-depth analysis often requires both measurement and simulation. Modelling may guide the measurement setup and requirements and may also be used to interpret the received signals [16]. Model-based signal processing of measured signals can be used to perform tasks such as dispersion compensation, phased array processing, and compensation of temperature induced fluctuations [17].

Rock bolts are used in mining and civil engineering to stabilize rock and prevent rock bursts. A study in one mine revealed that approximately 10 % of rock bolts were incorrectly installed even though the

* Corresponding author.
E-mail addresses: Philip.Loveday@wits.ac.za (P.W. Loveday), p.fromme@ucl.ac.uk (P. Fromme).

https://doi.org/10.1016/j.apacoust.2024.110262
Received 26 April 2024; Received in revised form 11 August 2024; Accepted 26 August 2024
Available online 30 August 2024
0003-682X/© 2024 The Authors. Published by Elsevier Ltd. This is an open access article under the CC BY-NC license (http://creativecommons.org/licenses/by-nc/4.0/).

installation was being observed [19]. Once the rock bolt has been installed, it is difficult to determine if it was correctly installed and after time it is difficult to determine if the rock bolt is still performing its function. It was noted in Villaescusa et al. [20] that pull-out tests are not applicable to grouted rock bolts and instead an over-coring technique was used to remove the rock bolt and surrounding rock. These are destructive tests, and a nondestructive test would be preferred. An overview of a broad range of nondestructive test methods for inspecting rock bolts was provided in Bačić et al. [10]. The use of ultrasonic guided waves is one of the approaches that has received considerable attention in recent years [21–24]. In pioneering work, Beard [21] investigated the use of both low and high frequency guided waves and proposed that the two frequency ranges may complement each other. Beard and Lowe [6] suggested that detecting rock bolts where the grouting is not complete or where corrosion of the rock bolt has occurred, causing the rod to be no longer completely bonded to the rock, would be best achieved by low frequency guided waves. Buys et al. [22] concentrated on low frequency guided waves, which are easier to investigate using numerical modelling and measurements. A prototype inspection instrument was developed as reported by Stepinski [23,25]. This instrument used low frequency guided waves (up to 100 kHz) with chirp signal excitation and made use of signal processing techniques to achieve longer distance detection. This prototype is an upgrade on the Boltometer instrument that was developed by Geodynamik [10] and which appears to be no longer available. Zima and Rucka [24] also used low frequencies (30–110 kHz) and showed some interesting diffraction effects where the rod enters the concrete.

Less research has been performed at high frequencies (1–10 MHz range), where many guided wave modes can propagate. Beard [21] showed that there is a succession of frequencies where different modes can propagate in an embedded rod with relatively low attenuation. At these mode and frequency combinations there is little motion of the outside radius of the embedded rod and therefore little leakage of energy into the grout and rock. This was demonstrated by measurements with a center frequency of 2.6 MHz for a 21.7 mm diameter embedded rod. Free rock bolts show a similar set of modes and frequencies where effective transmission of guided waves is possible at high frequencies [26]. Sun and Zhu [27] showed that the addition of surrounding concrete increases the attenuation but does not change the frequencies at which the attenuation minima occur. Therefore, measurements on a free rock bolt may be performed to determine suitable frequencies for testing an embedded rock bolt. Despite these efforts there are no commercial systems readily available for inspection of rock bolts and more research is required to find solutions to various inspection tasks. One of the simplest inspections would be to determine the length of an installed rock bolt to ensure that the correct lengths have been installed and that the bolt is not broken. Beard and Lowe proposed that this could be achieved using high frequency ultrasonic guided waves [6].

Like other guided wave measurements, measurements in rock bolts at high frequencies are complicated by the presence of numerous modes of propagation and large dispersion. These measurements typically require narrow frequency bandwidth signals, which are not available in standard equipment for ultrasonic testing. While some specialized research equipment is commercially available, the cost of this equipment makes it unattainable for many researchers and applications. This paper investigates what can be achieved with low-cost measurement equipment, which would be available to most researchers and could be economically viable in industrial applications. A system based on traditional bench-top arbitrary waveform generator and oscilloscope and a system based on a USB oscilloscope, which includes an arbitrary waveform generator, are compared in terms of price and performance. The performance is quantified by the signal-to-noise ratio (SNR), and the influence of averaging, filtering, and pre-amplification is investigated. The systems were not intended for measurements on rock bolts installed in a mine but are suitable for laboratory investigations.

Section 2 provides a brief background on rock bolts and the ultrasonic guided wave propagation in cylinders, which informs the measurement system requirements. The two measurement systems used in this research are described in Section 3. Section 4 contains a comparison of the SNR of the two systems and an investigation of the influence of signal processing and hardware selections on the signals that can be detected. Conclusions and recommendations from this study are presented in section 5.

2. Ultrasonic guided wave propagation in rock bolts

An overview of different types of rock bolts used in mining was provided by Peter at al. [18]. Grouted rock bolts are common and the installation of these is briefly described. A hole of approximately 30 mm diameter is drilled into the rock face and the bolt (diameter 22–25 mm) is embedded in the hole either with concrete grout or an epoxy resin. A plate and nut are added at the exposed end of the rod, and the plate is tightened against the rock face to support the rock. The rock bolt is generally a deformed round bar, similar to those used in reinforced concrete, with a threaded section at the exposed end. The embedded end of the rock bolt is often cut at a 45-degree angle. The functions of the grout are to mechanically attach the bolt to the rock and to prevent ground water from causing corrosion of the bolt [18].

The design of a guided wave ultrasound measurement begins with a selection of the mode or modes of propagation and frequency range of operation. This selection is based on the nature of the propagation of guided wave modes in the structure which can be determined by analytical or numerical modelling. The propagation of guided waves in infinite cylinders may be computed by numerical solution of the Pochhammer-Chree frequency equation [28]. This numerical solution is implemented in the free software PCDISP [28] and may be used to compute dispersion characteristics of multi-layered cylinders. Beard [21] modelled free rods as well as rods embedded in rock with different grouting layer properties using the commercially available Disperse software [29].

The phase and group velocity dispersion curves of axisymmetric modes in a 20 mm diameter steel rod are plotted in Fig. 1, which was generated using the free software PCDISP, which is a MATLAB code by the authors of [28]. This software uses the analytical solution of the 3D elastic wave equation in a multi-layered cylinder. The software allows for all of the longitudinal modes to be labelled and identified based on their respective cut-off frequencies, but for clarity only the L(0,27) mode is labelled in Fig. 1b at the frequency where its group velocity is a maximum. It must be noted that the physical properties of the rock bolt sample, which was tested, are not accurately known. The properties used in the computation were Young's modulus of 210 GPa, Poisson's ration of 0.29, and density of 7950 kg/m^3. Measurements will be performed between 4 and 6 MHz, which is a higher frequency than used by previous researchers. Fig. 1b shows that there are many propagating modes in the frequency range between 4 and 6 MHz. Each consecutive mode has its maximum group velocity at a higher frequency. A mode with a high group velocity is attractive for inspections, as this mode arrives first, making it easier to identify in a complex signal. The properties used in the model were selected, within the range of expected properties, to align the frequencies of the peak velocities with the frequencies of peak amplitude response measured later.

The group velocity is seen to change with frequency but remains relatively constant over a narrow frequency range. Unlike conventional ultrasonic testing, where a short, broadband excitation signal is used, the excitation of guided waves most commonly uses narrowband tone burst signals. These signals typically consist of several cycles of a sine wave windowed by a Hann window as illustrated in Fig. 2. The center frequency of this signal coincides with the frequency of the sine wave while the frequency bandwidth is determined by the number of cycles with more cycles reducing the bandwidth. When a Hann window is used, the bandwidth of the signal may be estimated by multiplying the center frequency by 4 and dividing by the number of cycles [15]. A narrow-

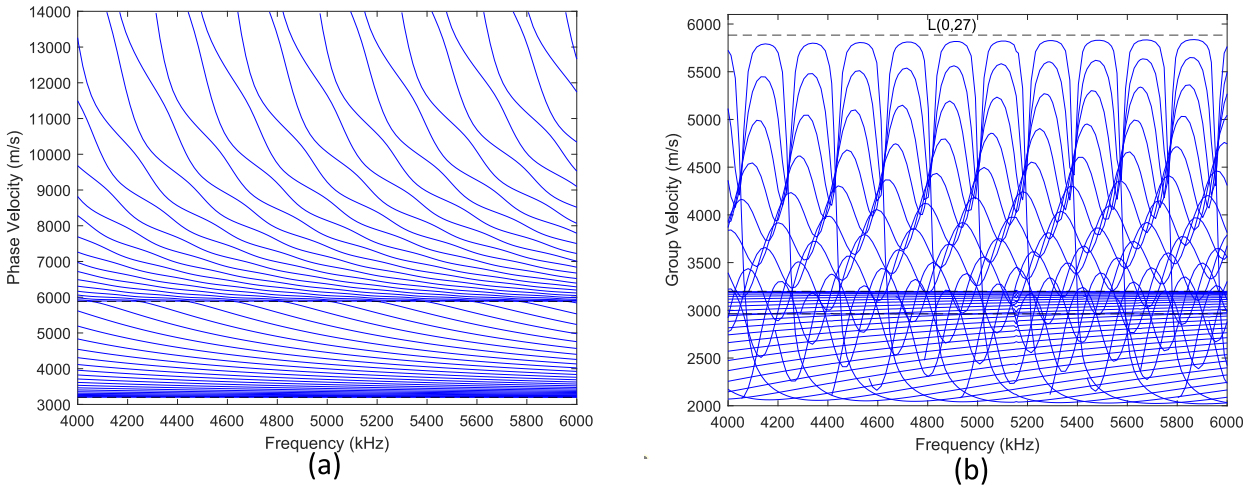


Fig. 1. (a) Phase and (b) group velocity dispersion curves of axisymmetric modes of propagation in a 20 mm diameter steel rod.

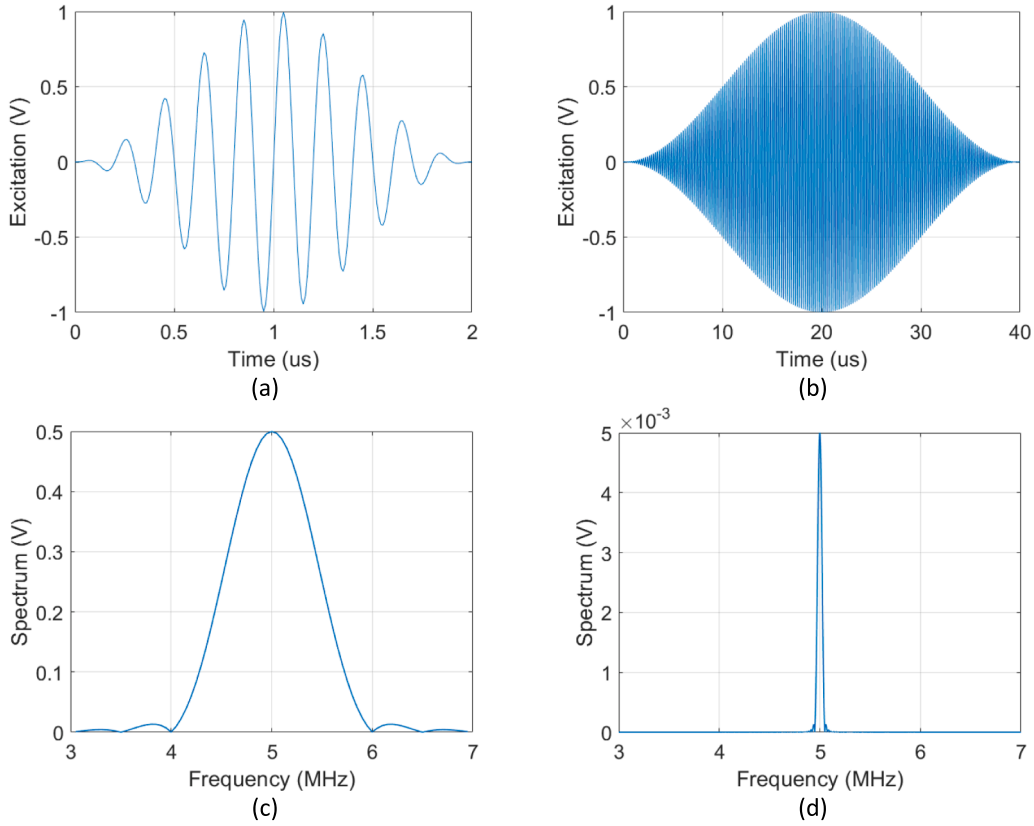


Fig. 2. Tone burst excitation signals with 5 MHz center frequency: (a) 10 cycles; (b) 200 cycles; frequency spectrum of signal with: (c) 10 cycles (bandwidth 2 MHz); (d) 200 cycles (bandwidth 0.1 MHz).

band signal is suitable for excitation of a specific mode in a rock bolt at the highest group velocity. The generation of these signals requires a programable function generator.

3. Equipment

The equipment used is shown in Fig. 3 and the individual items and estimated costs are listed in Table 1. A 1 m long section of a rock bolt having 20 mm diameter was tested. This section included the free end of the rock bolt, which was threaded, and the remainder of the specimen is deformed bar (having mixing ribs), i.e., the test specimen is not of constant circular cross-section as modeled in Section 2. It was noted by Beard [21] that these surface features do not cause detectable reflections of the guided wave modes of interest, as the mode shapes have energy concentrated at the center of the cross-section with little motion at the outer surface of the rod and are therefore largely insensitive to features located there. The approximation as a cylinder with constant, circular cross-section is therefore acceptable in this study. Both ends of the rock bolt section were machined flat for attachment of the ultrasonic transducers. The transducers used were 5 MHz ultrasonic testing probes for introducing longitudinal waves, with an active element diameter of 6 mm. These transducers were available and could easily be substituted by

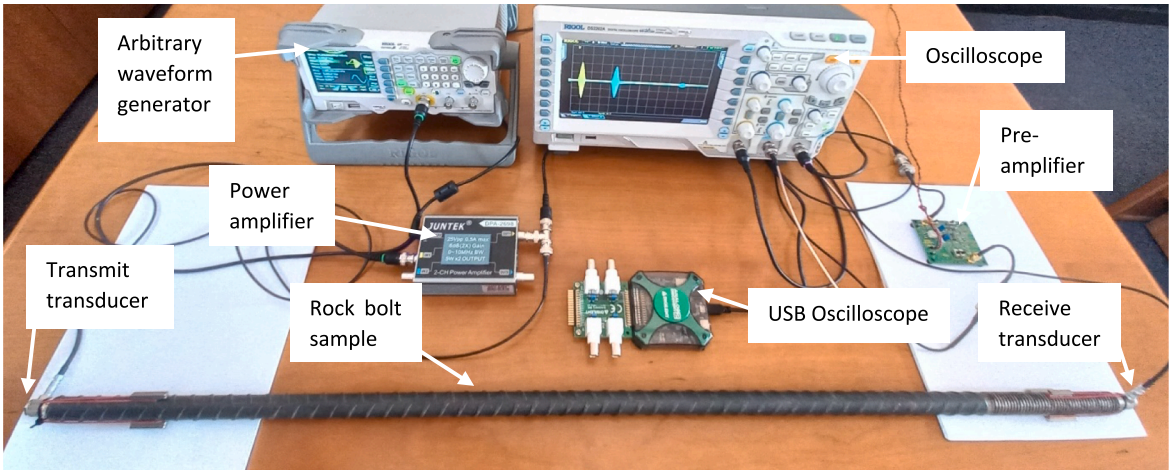


Fig. 3. Photograph of equipment used in measurements.

Table 1
Equipment and Cost Estimates.

Item	Make/Model/Specifications	Cost (USD)	Cost (USD)
Two piezoelectric ultrasonic transducers and cables	SIUI P5-6L 5 MHz transducers with 6 mm diameter active element	600	600
Power amplifier	Juntek DPA-2698	75	75
Pre-amplifier	AD8331 Evaluation Board	105	105
Bench-top arbitrary waveform generator	Rigol DG1022Z	540	
Bench-top oscilloscope	Rigol DS2202A	660	
USB oscilloscope/arbitrary waveform generator	Digilent AD2 Pro Bundle		330
Total Cost		**1980**	**1110**

1, 2 or 10 MHz ultrasonic testing probes if measurements are required at lower or higher frequencies. The cost estimate of USD 600 includes two ultrasonic contact transducers and cables (BNC to Lemo connectors). Initially measurements were performed with ultrasonic coupling gel between the transducers and the rock bolt sample. The signals obtained varied over time and were very sensitive to the transducer attachment. The ultrasonic coupling gel was replaced with liquid honey and larger first arrival signals with better repeatability and stability were obtained. The transducers were held in place by elastic bands and magnets on the rock bolt. All measurements were performed in transmission mode by transmitting on one transducer and receiving on the other transducer. The power amplifier used was a small amplifier that is used to amplify signals from a function generator. The amplifier has a 10 MHz bandwidth but is limited to a maximum voltage excitation of 25 Vpp and 5 W of power per channel. A more powerful amplifier would be advantageous, but these tend to be large and expensive instruments. Measurements were performed initially by connecting the receive transducer directly to the oscilloscope. The influence of adding a pre-amplifier on the receive side was investigated using an evaluation board from Analog Devices. The evaluation board is based on the AD8331 ultralow noise variable gain amplifier, which has an output-referenced noise of 48 nV/$\sqrt{\text{Hz}}$ according to the datasheet. Using an evaluation board provided a low noise pre-amplifier at a low-cost.

The measurements using bench-top instruments were performed using a Rigol DG1022Z arbitrary waveform generator and a Rigol DS2202A digital oscilloscope. These instruments were selected as good value for money with acceptable performance and extensive features. The Rigol arbitrary waveform generator had 14-bit resolution, sample rate of 200 million samples per second (MSa/s), output range of ±5 V and memory of 2 million points. The Rigol oscilloscope had 8-bit resolution with a minimum range of 0.5 mV/div. The analog bandwidth was 200 MHz and 28 million measurement points could be stored. The input impedance used was 1 MΩ in parallel with 16 pF. The oscilloscope also offered the option of 50 Ω input impedance but selecting this resulted in a poorer signal-to-noise ratio. Specifications for the noise performance of the oscilloscope could not be found. The averaging performed on the bench-top oscilloscope only averaged what is shown on the display so averaged signals could not be captured for later processing. Instead, multiple signals were captured and then averaged on a computer. This increased the time required for the measurements.

In the measurements with the USB oscilloscope, both Rigol instruments were replaced by the Digilent Analog Discovery 2, which includes an arbitrary waveform generator. This instrument was selected as a low-cost device that could perform the required functions in one instrument. The arbitrary waveform generator had 14-bit resolution with a 100 MSa/s sampling rate, 20 MHz bandwidth and an output range of ±5 V. The USB oscilloscope had 14-bit resolution over a range of ±25 V, 100 MSa/s sampling rate and a bandwidth of 20 MHz. The input impedance of the USB oscilloscope was 1 MΩ in parallel with 24 pF. Specifications for the noise performance could not be found. More USB oscilloscopes are appearing on the market and there are several other manufacturers that the authors are aware of. The purpose of this investigation was not to perform an exhaustive comparison of USB oscilloscopes and only the instrument that appeared to offer adequate performance (for this application) at the lowest cost was considered.

The measurement systems investigated only allowed transmission mode measurements to be performed. The transmission mode measurements may be used to research the propagation, scattering, attenuation, transmission, and reception of the guided waves to generate knowledge that would allow an inspection instrument to be developed in future. Installed rock bolts would require pulse-echo measurements to be performed from the exposed end of the rock bolt and would require additional electronics to use a single transducer for transmitting and receiving the signals. The measurement of rock bolts installed in a mine was outside the scope of this study.

As shown in Table 2, the total cost of the system based on the bench-top instruments was estimated at USD 1980 while replacing the bench-top instruments with the USB oscilloscope reduced the estimated cost to USD 1110. The contact ultrasonic transducers were a significant portion of the total cost and cheaper alternatives or purchasing online could reduce this cost. Both systems are considered to be low-cost systems and they are believed to cost at least an order of magnitude less than commercially available systems generally being used for ultrasonic guided wave research. It is believed that the costs listed in Table 2 would be acceptable to most researchers and for most applications.

Table 2
Predicted peak group velocity frequencies and measured peak amplitude frequencies. Mode numbering of axisymmetric modes based on cut-off frequencies over full frequency range.

Mode	L(0,24)	L(0,25)	L(0,26)	L(0,27)	L(0,28)	L(0,29)	L(0,30)	L(0,31)	L(0,32)
Predicted Peak Group Velocity Frequency (MHz)	4.340	4.535	4.723	4.910	5.105	5.293	5.480	5.676	5.863
Measured Peak Amplitude Frequency (MHz)	4.360	4.550	4.735	4.925	5.095	5.280	5.450	5.650	5.840

4. Results

Measurement results are presented in this section for a 1 m free rock bolt, received at the opposite end to the guided wave excitation. Firstly, the influence of the parameters of the excitation signal was considered. The number of cycles and the center frequency were varied, and the results obtained were compared to the theory presented in Section 2. Secondly, a comparison was made between the performance of the two oscilloscopes. Finally, the influence of a pre-amplifier and transducer electrical impedance matching were investigated.

4.1. Influence of number of cycles and center frequency of tone burst excitation

Measurements were performed with tone burst signals containing 10 and 200 cycles with a center frequency of 4.925 MHz, similar to those illustrated in Fig. 2a and b, respectively. This center frequency was selected as it produced a maximum response and was close to the nominal operating frequency of the ultrasonic transducers. For comparison purposes measurements with a rectangular pulse, similar to what would be used in convention ultrasonic testing, were performed. The pulse was selected to have a center frequency of 4.925 MHz. These measurements were performed using the bench-top equipment and a

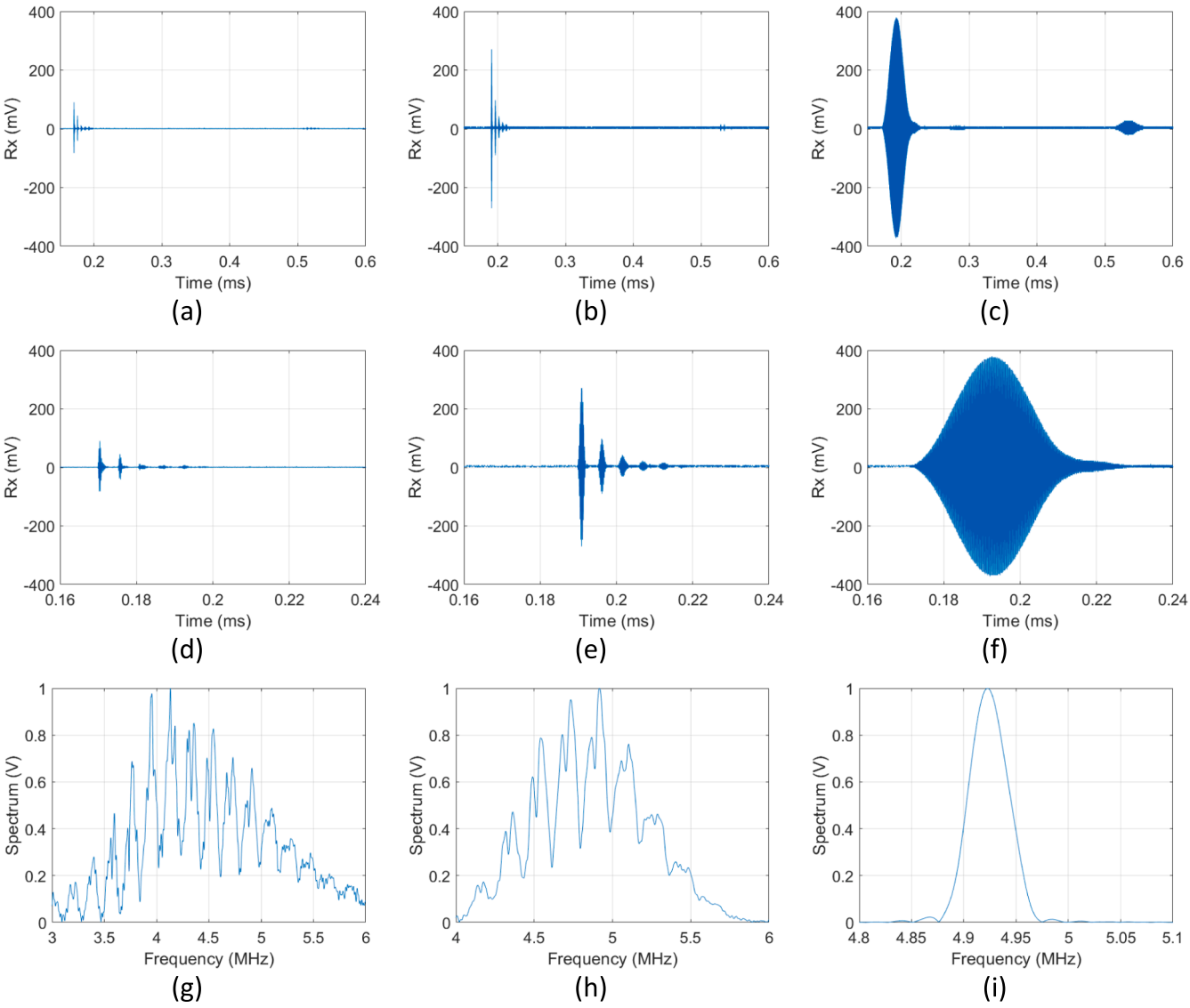


Fig. 4. Influence of number of cycles excitation signal on response signal, (a) rectangular pulse, 1st two arrivals, (b) 10 cycles, 1st two arrivals, (c) 200 cycles, 1st two arrivals, (d) rectangular pulse zoomed view, (e) 10 cycles zoomed view, (f) 200 cycles zoomed view,(g) frequency spectrum of 1st arrival for rectangular pulse excitation signal, (h) frequency spectrum of 1st arrival for 10-cycle excitation signal, (i) frequency spectrum of 1st arrival for 200-cycle excitation.

sampling rate of 100 MSa/s. In Fig. 4a, 4b, and 4c the responses to the rectangular pulse, 10-cycle tone burst, and 200-cycle tone burst signals are shown. The timescale selected in these graphs covers the first and second arrivals of the signals at the receiving end of the rock bolt. The graphs in Fig. 4d, e, and f show the same results but zoomed to show only the first arrival. It is evident that when the rectangular pulse and the 10-cycle tone burst excitations are applied, the signal arrives as a succession of wave packets for each arrival. The bandwidth of these excitation signals is large enough to cover several different peaks of group velocity in the dispersion plots, corresponding to different guided wave modes (Fig. 1). It was explained by Beard [21] that the response of a single mode includes dispersion and the received wave packet for a single mode would be significantly longer than the excitation signal. As the excitation signal would excite several modes around their group velocity maxima, the measured response is the sum of the responses of the individual modes and constructive and destructive interference causes the sum to contain the multiple short duration wave packets observed in Fig. 4d and e. The FFT of the first arrival, for the rectangular pulse and the 10-cycle tone burst excitation is shown in Fig. 4g and h, where several peaks corresponding to the peak frequencies of the different guided wave modes predicted in Fig. 1 can be observed. The rectangular pulse contained energy between 3 MHz and 6 MHz while the 10-cycle tone burst contained energy between 4 MHz and 5.5 MHz. The bandwidth of the 200-cycle tone burst is much smaller (approximately 0.1 MHz, Fig. 2d, Fig. 4i) and approximately matches the high group velocity plateau of a single mode (L(0,27)), so other modes are not excited at their group velocity maxima. The response to the 200-cycle tone burst excitation signal shows only limited dispersion and illustrates the need for narrow frequency band excitation in this application. Limiting the frequency bandwidth of the excitation signal avoids exciting modes outside this frequency range. There are, however, mode with lower group velocity within the frequency range that is excited, and the response can be multi-modal. These lower group velocity modes would arrive later and be spread out in time, as these modes have significant dispersion and are not clearly visible in the response, which is dominated by the highest group velocity mode with lowest dispersion.

Measurements were performed, with the bench-top equipment, with the 200-cycle tone burst and with varying center frequency. The center frequency was adjusted by changing the sampling rate on the arbitrary waveform generator and the frequencies at which peak amplitudes of the response were obtained were recorded. The amplitude of response of a particular mode increases rapidly at first when the frequency is adjusted but in the vicinity of the peak amplitude there is little sensitivity of the amplitude to small frequency changes as would be expected from the shape of the peaks in Fig. 1. This makes it difficult to accurately measure the frequency at which the peak occurs. The results are shown in Table 2 and good agreement between the spacing of the measured peak amplitude frequencies and the predicted group velocity peaks is evident. The largest response was obtained when the center frequency of the excitation signal was set to 4.925 MHz, which corresponds to mode L(0,27). This mode had low attenuation allowing multiple arrivals to be detected and this frequency was used for later experiments in this study. This result shows that the frequencies for inspection can be determined on a free rock bolt by using this equipment. The predicted group velocity maxima for the modes listed in the table ranged from 5800 m/s (for mode L(0,24)) to 5838 m/s (for mode L(0,32)). The group velocities estimated from the measurements for these two modes were 5858 m/s and 5876 m/s, which are in good agreement (1 % difference) with the predicted values.

4.2. Comparison of benchtop and USB oscilloscopes

When using the two oscilloscopes it was noticed that the noise present in the measurement using the USB oscilloscope was greater than that observed with the bench-top equipment. The sampling rate of both oscilloscopes was set to 100 MSa/s for this measurement. The bench-top oscilloscope captured 70,000 samples while the USB oscilloscope could only capture 8192 samples (2 channels), which meant that a shorter length of signal was captured and the frequency resolution after application of the Fast Fourier Transform (FFT) would be lower. Averaging is commonly used in guided wave ultrasound measurements to reduce the random noise in the measured signals (inversely proportional to square root of the number of averages). Noise measurements for the two systems are shown in Fig. 5. These measurements were performed with the excitation signals and the power amplifier connected and powered. The noise was measured over a time interval long after the excitation was applied to make sure that no ultrasonic energy remained. We are not interested in DC offsets and the mean of these measurements was subtracted from the measurements before they were plotted to make comparisons easier. Note that the vertical scale for the USB oscilloscope measurements (Fig. 5b) is 20 times larger than that used for the bench-top measurements (Fig. 5a). The zoomed views in Fig. 5c and d show the response over a shorter time period, and the digitization levels of the two oscilloscopes are visible. These results illustrate the noise reduction that can be obtained by averaging. The root mean square (RMS) of the signals was calculated after the mean of the signals had been subtracted. These values are listed in Table 3. It is seen that the 100 averages reduced the RMS of the noise by approximately ten times as expected. The RMS noise on the bench-top oscilloscope is approximately 25 times lower than the RMS noise on the USB oscilloscope.

The frequency spectra of the noise signals, in the frequency range of interest, were computed using FFT and are plotted in Fig. 6a and Fig. 6b. Once again, the influence of the averaging is clear as is the greater noise level from the USB oscilloscope compared to the bench-top instruments. The noise is distributed over the frequency range of interest and in the case of the bench-top equipment there are evenly spaced peaks in the spectrum. The source of this noise is believed to be the power amplifier used as these peaks disappeared when the power amplifier was switched off. These peaks are not visible in the spectrum from the USB oscilloscope because the noise is greater than these peaks. When the 200-cycle tone burst signals are used, the energy is concentrated in a bandwidth of approximately 100 kHz. We therefore only need to consider this bandwidth and we can eliminate noise that falls outside of this frequency range. This bandpass filtering was performed by transforming the signals to the frequency domain, zeroing all content outside of the frequency range 4.875 MHz to 4.975 MHz (for a signal with center frequency of 4.925 MHz), and converting back to the time domain. This bandpass filtering can have a significant effect on the noise as shown in the graphs in Fig. 6c for the bench-top oscilloscope and Fig. 6d for the USB oscilloscope. The RMS values of the noise signals shown in Fig. 5 and Fig. 6 are listed in Table 3, showing the effectiveness of both averaging and bandpass filtering for reducing the noise in the measurements. The filtering was particularly effective on the signals captured with the USB oscilloscope. After filtering, the noise in the signals captured by the USB oscilloscope was approximately four times greater than the noise in signals captured by the bench-top oscilloscope. Further reduction in the noise levels could be achieved by taking a greater number of averages, although this would increase the time required for the measurements. If a further decrease of ten times is required, the average of 10 000 samples could be used. This would increase the measurement time by 99 times. Excitation signals with more cycles could be used to decrease the bandwidth of the signals further. Depending on the application, this may not be desirable as spatial resolution would be compromised due to the increased time duration of the wave packet.

Measurements of the first three arrivals (excitation signal containing 200 cycles with center frequency of 4.925 MHz), using the two oscilloscopes, are presented in Fig. 7. The amplitude of the arrivals decreases by approximately a factor of 20 times for each arrival. When the ultrasonic coupling gel was used instead of the honey the amplitude of the arrivals decreased by approximately a factor of 10 times for each arrival. The superior coupling of the transducer by the honey results in more

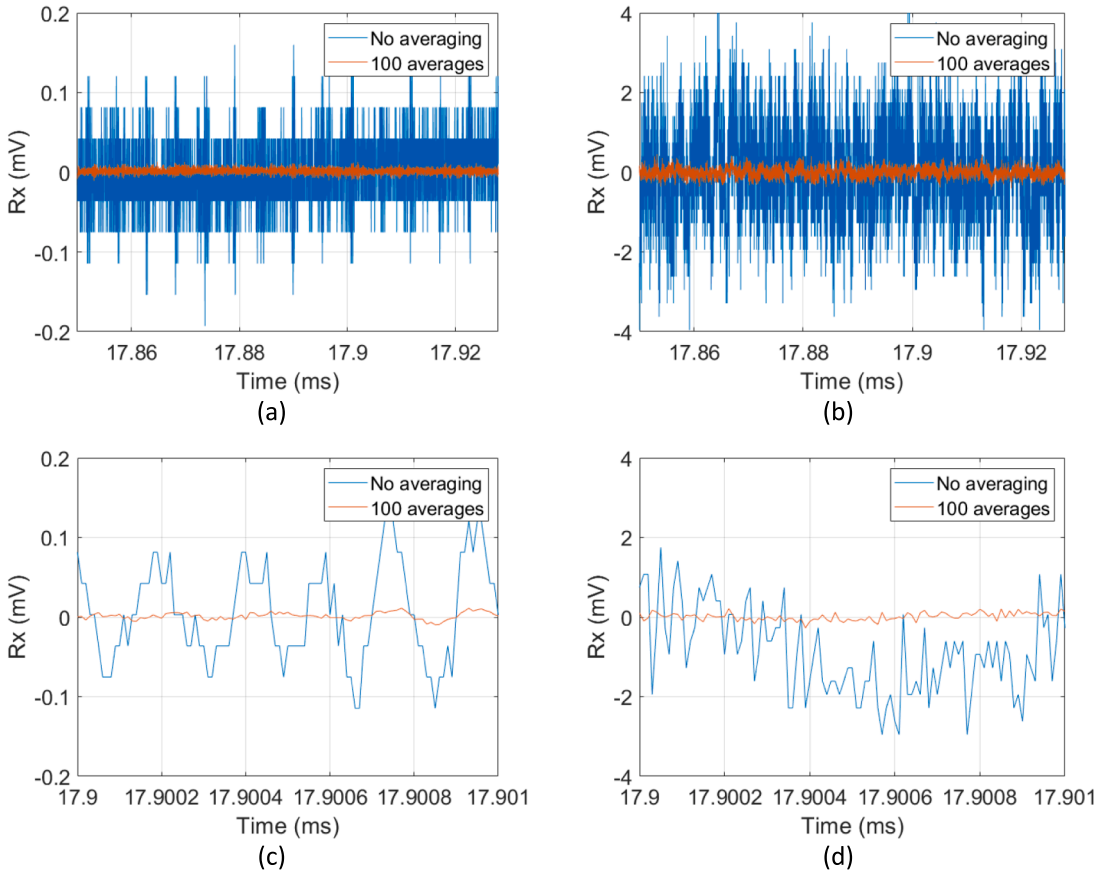


Fig. 5. Comparison of noise measured by (a) bench-top oscilloscope, (b) USB oscilloscope, (c) zoomed view of noise measured by bench-top oscilloscope, (d) zoomed view of noise measured by USB oscilloscope.

Table 3
RMS noise values for the two oscilloscopes and the influence of averaging and bandpass filtering.

RMS noise (μV)	Bench – top oscilloscope	USB oscilloscope
1 average	40.91	1161.1
100 averages	3.74	122.2
100 averages and band pass filtering	0.99	3.93

energy dissipated in the transducer at each reflection. The results show the higher noise in the USB oscilloscope, which makes measurement of smaller signals difficult. The 3rd reflection can be easily observed in the measurement performed with the bench-top oscilloscope (Fig. 7e), while it is hidden by noise in the measurement performed using the USB oscilloscope (Fig. 7f). Using an average of 100 measurements (Fig. 7h) made the 3rd arrival visible when the USB oscilloscope was used.

4.3. *Influence of pre-amplification and impedance matching*

An inexpensive pre-amplifier (AD8331 Evaluation Board) was used to amplify the signal received by the transducer before it was measured by the oscilloscopes. Passive electrical impedance matching, using inductors and capacitors, was used to improve the matching of the transmit transducer to the power amplifier and the receive transducer to the pre-amplifier following the procedures in Petersen [30]. The influence of the pre-amplifier and the impedance matching were measured and are shown in the graphs in Fig. 8 for the 200-cycle excitation signal. The signal and noise RMS values were calculated for these measurements and are listed in Table 4. Measurements were performed before the pre-amplifier was added and after the pre-amplified was added. Fig. 8a and b show the 3rd reflection, measured using both oscilloscopes, without the pre-amplifier. This measurement was performed with 100 averages and the noise is clearly visible in the measurement performed with the USB oscilloscope. This noise is significantly reduced by filtering the frequencies outside of the range 4.875 to 4.975 MHz. Noise measurements (long after the excitation) were performed with the two oscilloscopes without the pre-amplifier as shown in Fig. 8c and d. The vertical scale of these two graphs is the same to show the significant difference in noise.

Measurements of the third arrival with the pre-amplifier are shown in Fig. 8e and f. The gain of the pre-amplifier was estimated to be approximately 31.5 dB (a gain of 38 times) by comparing these measurements to those performed without the pre-amplifier. The influence of the noise on the measurement with the USB oscilloscope was reduced by including the pre-amplifier (Fig. 8f compared to Fig. 8b). The noise measured using the two oscilloscopes with the pre-amplifier included is shown in Fig. 8g and h. It is seen, by comparing Fig. 8c with g, that the noise for the bench-top oscilloscope increased significantly (33 dB) when the pre-amplifier was added. The noise for the USB oscilloscope did increase but only by a relatively small amount (8 dB) when the pre-amplifier was added (compare Fig. 8d with f). This indicates that a large portion of the noise measured by the USB oscilloscope (without the pre-amplifier) was generated within the oscilloscope and therefore did not increase as much when the pre-amplifier was added. The addition of the electrical impedance matching increased the amplitude to the signal, measured by the bench-top equipment, by approximately 14.5 dB or 5.3 times (compare Fig. 8e and i). However, the increase in noise was similar (compare Fig. 8g and k). The measurements performed with the USB oscilloscope showed a similar increase in signal when the impedance

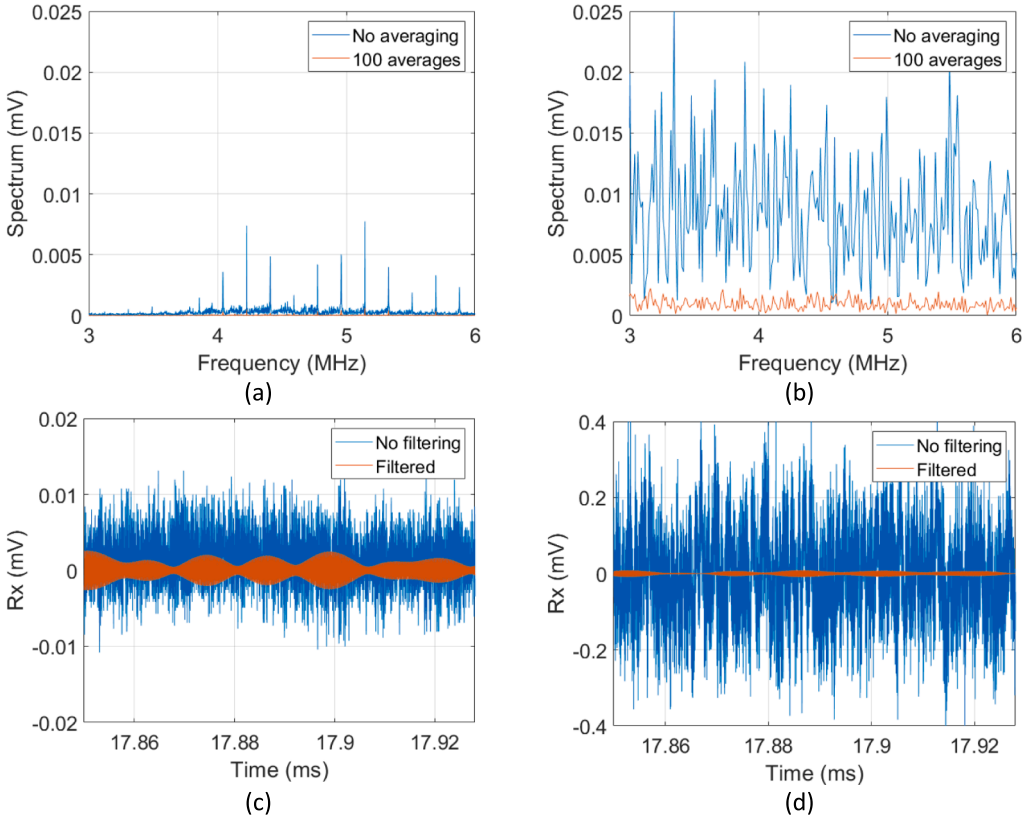


Fig. 6. Frequency content of noise signals (a) measured with bench-top oscilloscope and (b) measured with USB oscilloscope. Influence of bandpass filtering on signals from (c) bench-top oscilloscope and (d) USB oscilloscope.

matching was added but the noise did not increase as much resulting in an improved signal to noise ratio.

The signal, noise, and signal to noise ratio for the different cases are listed in Table 4. These results are based on signals after 100 averages, without and with frequency bandpass filtering. The RMS value of the arrival signals was calculated by measuring the peak amplitude of the wave packet and multiplying this by 0.7071 as we are interested in the amplitude of the peak of the signal. The RMS value of the noise signals was computed in the usual way. The signal to noise ratio is defined as the ratio of the power of the arrival signal to the power of the noise signal, therefore the ratio of the RMS values was squared to obtain this value. The table shows that the noise increased significantly when the pre-amplifier was added, when measured by the bench-top oscilloscope, but not when measured by the USB oscilloscope as mentioned previously. This is also the case for the results after filtering.

For both oscilloscopes, the addition of electrical impedance matching increased the magnitudes of the received signals. When the bench-top instruments were used, the addition of the matching increased the noise and had little influence on the SNR. The addition of the matching produced a smaller increase in the noise when the USB oscilloscope was used and in this case the matching improved the SNR (about factor 4). When bandpass filtering was included the influence of the matching on the SNR was less substantial for the USB oscilloscope (about factor 3). When the bandpass filtering was used with the bench-top instruments the addition of the matching decreased the SNR (factor 2). When the bench-top instruments were used, the best SNR was obtained with the pre-amplifier and the bandpass filtering and this performance was comparable to that of the USB oscilloscope with the pre-amplifier, impedance matching and bandpass filtering.

4.4. *Measurement of guided wave signals with long propagation distance*

The ability of the measurement system to detect later arrivals of the wave packet is determined by the SNR of the system. The noise for various setups was quantified in the previous section. It was noted that the signal for each consecutive arrival decreases by a factor of approximately 20. This decrease in signal amplitude is caused by attenuation (damping) of the waves as they propagate along the rock bolt, dispersion of the waves causing the wave packet to become elongated and therefore smaller, and imperfect reflection of energy in the mode of propagation at the ends of the rock bolt. The reflection of the energy at the ends of the rock bolt could include mode conversion where some of the incident energy is reflected as other modes of propagation, which are then attenuated as they propagate. Some of the incident energy is transferred from the rock bolt to the piezoelectric transducers, which allows the waves to be measured. It was found that the use of honey to couple the transducers to the rock bolt produced a larger first arrival compared to that obtained when ultrasonic coupling gel was used. This improved coupling resulted in greater transfer of energy to the transducers at each reflection and each consecutive arrival at the receiver end was approximately a factor of 20 smaller. When the ultrasonic coupling gel was used the consecutive arrivals were approximately a factor of 10 times smaller. For detecting later arrivals, the use of ultrasonic coupling gel was therefore preferred. Measurements were performed with the two oscilloscopes to detect the fifth arrival, equivalent to a propagation distance of 9 m (approximately 9000 wavelengths) with multiple reflections along the rock bolt. Fig. 9 shows the signals captured by the two oscilloscopes using 100 averages and the pre-amplifier and impedance matching. The fifth arrival was detected and the performance of the two oscilloscopes was similar. The sixth arrival could not be detected. If the excitation voltage could be increased, by the use of a more powerful amplifier, it may be possible to detect the sixth arrival.

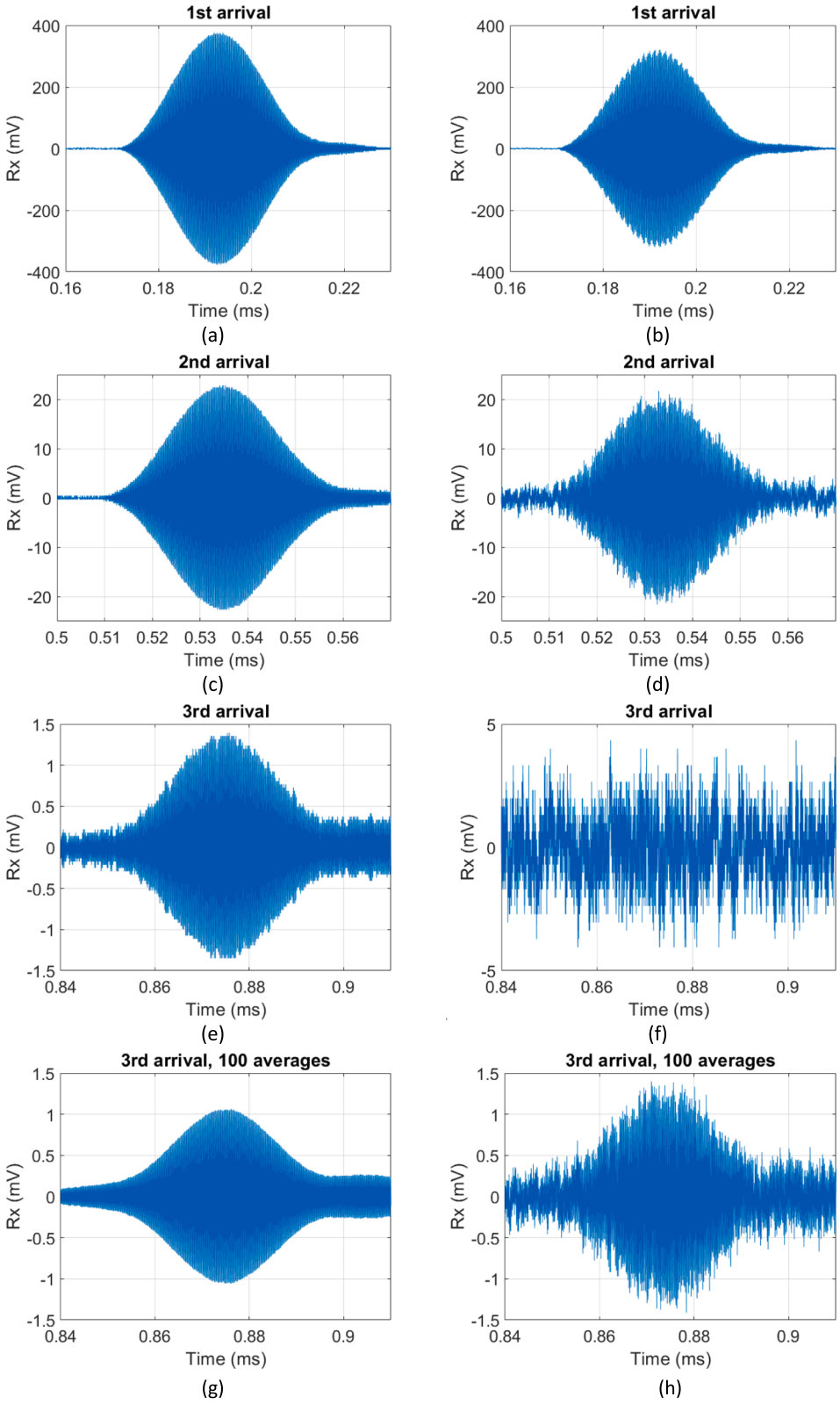


Fig. 7. Comparison of first three arrivals (200 cycles excitation signal) measured with bench-top instruments and USB oscilloscope. (a), (c), and (e) 1st, 2nd and 3rd arrivals with bench-top instruments, (b), (d), and (f) 1st, 2nd and 3rd arrivals with USB oscilloscope, (g) 3rd arrival and 100 averages with bench-top instruments, (h) 3rd arrival and 100 averages with USB oscilloscope.

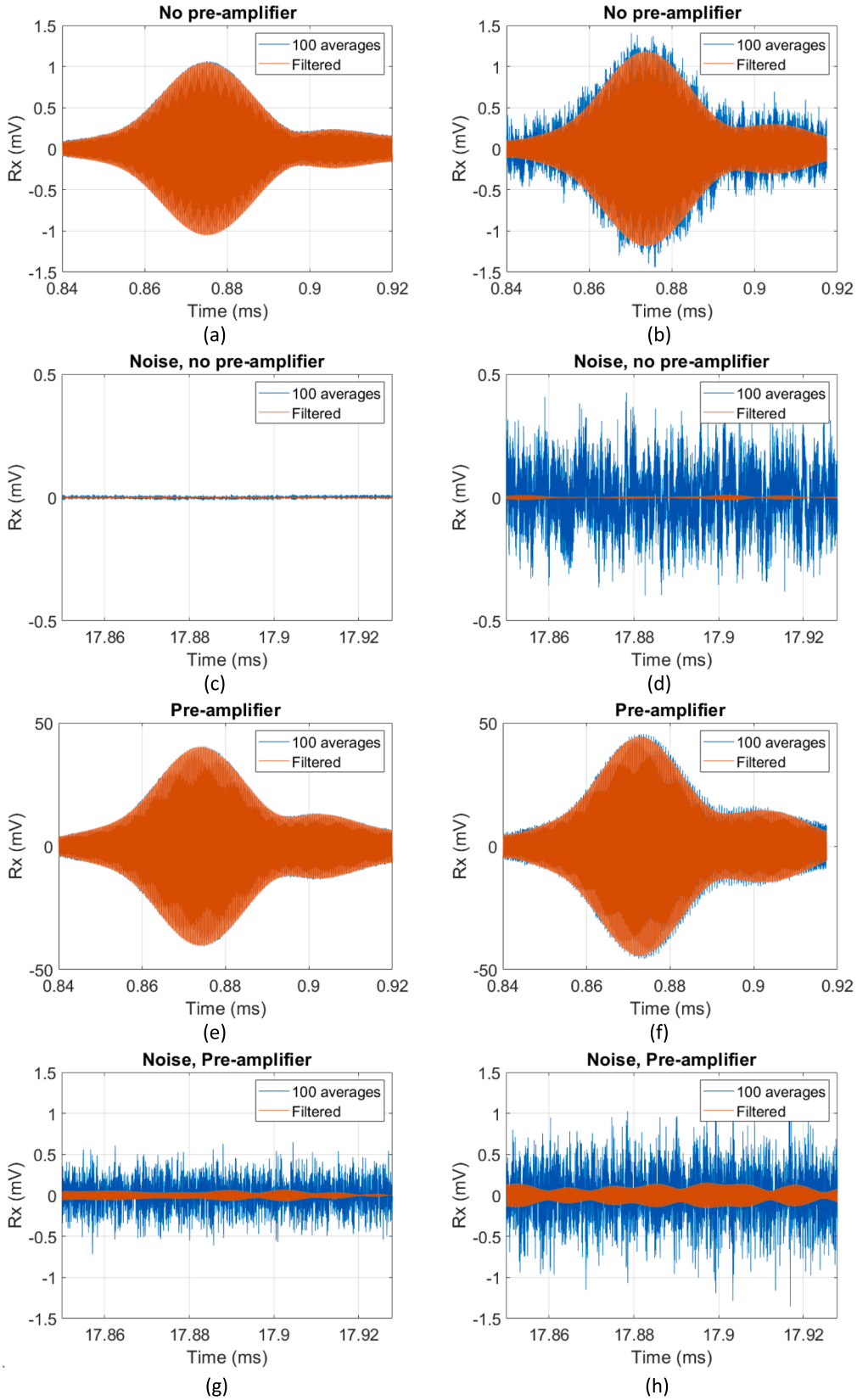


Fig. 8. Influence of pre-amplifier with gain of 33 dB on signals (200 cycles excitation signal) measured using bench-top instruments (a, c, e, g, I, k) and USB oscilloscope (b, d, f, h, j, l). All measurements performed with 100 averages and influence of bandpass filtering shown. (a, b) third arrival, no pre-amplifier; (c, d) noise, no pre-amplifier; (e, f) third arrival, pre-amplifier; (g, h) noise, pre-amplifier; (i, j) third arrival, matching and pre-amplifier; (k, l) noise, matching and the pre-amplifier.

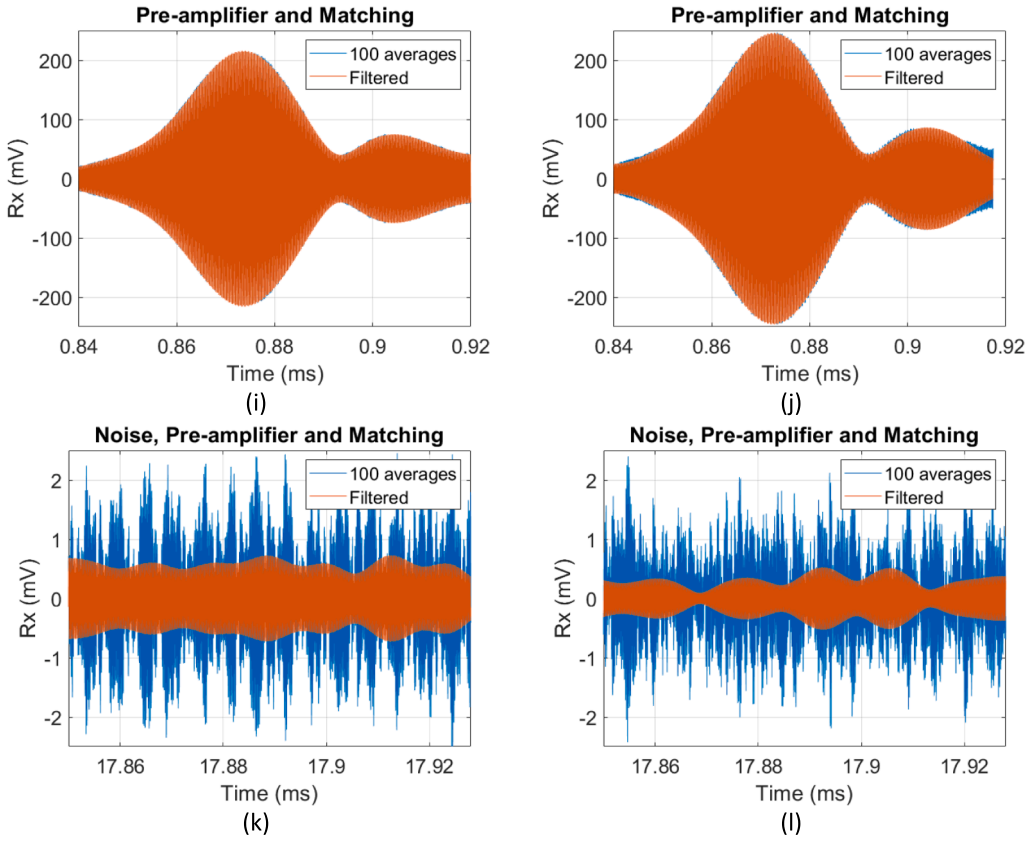


Fig. 8. (*continued*).

Table 4
SNR for two oscilloscopes and influence of pre-amplification and matching.

		Bench-Top Oscilloscope			USB Oscilloscope		
		RMS Signal (V)	RMS Noise (V)	SNR	RMS Signal (V)	RMS Noise (V)	SNR
No filter	No pre-amp	7.46 x 10^{-4}	4.04 x 10^{-6}	3.42 x 10^{4}	8.40 x 10^{-4}	1.18 x 10^{-4}	5.06 x 10^{1}
No filter	Pre-amp	2.86 x 10^{-2}	1.82 x 10^{-4}	2.47 x 10^{4}	3.15 x 10^{-2}	2.98 x 10^{-4}	1.12 x 10^{4}
No filter	Pre-amp and matching	0.153	9.29 x 10^{-4}	2.71 x 10^{4}	0.174	7.14 x 10^{-4}	5.99 x 10^{4}
Filtered	No pre-amp	7.46 x 10^{-4}	2.99 x 10^{-6}	6.24 x 10^{4}	8.40 x 10^{-4}	5.08 x 10^{-6}	2.73 x 10^{4}
Filtered	Pre-amp	2.86 x 10^{-2}	5.08 x 10^{-5}	3.16 x 10^{5}	3.15 x 10^{-2}	1.09 x 10^{-4}	8.39 x 10^{4}
Filtered	Pre-amp and matching	0.153	6.16 x 10^{-4}	6.17 x 10^{4}	0.174	3.36 x 10^{-4}	2.71 x 10^{5}

These measurements were repeated using the rectangular pulse and the 10-cycle tone burst excitation signals with the bench-top instrumentation. It was possible to detect the fourth arrival when the 10-cycle tone burst was used and only the third arrival when the rectangular pulse was used. This demonstrated that more narrowband and thus longer excitation signals, which contain more energy concentrated in as few guided ultrasonic wave modes as possible, offer advantages when long range propagation is required.

5. Conclusions and recommendations

A low-cost setup was investigated to measure high frequency ultrasonic guided waves in a section of a rock bolt. It was possible to confirm some modeling predictions for high frequency guided wave propagation using this low-cost equipment. This indicated the frequencies that would be suitable for performing inspections. The fifth arrival, which was approximately 80 dB smaller than the first arrival could be detected by using a 200-cycle tone burst excitation signal. This corresponds to a propagation distance of approximately 9000 wavelengths (9 m).

Two different types of instrumentation were compared. A traditional bench-top oscilloscope and bench-top arbitrary waveform generator were used in the first case. A USB oscilloscope, which included an arbitrary waveform generator, was used in the second case. It was observed that the bench-top oscilloscope had significantly less noise than the USB oscilloscope, which was initially considered an advantage. It was found that the addition of a pre-amplifier made the noise level of the USB oscilloscope less important and ultimately the two devices performed similarly. The USB oscilloscope had limited memory so only relatively short time durations could be captured with a sampling rate of 100 MSa/s. The bench-top oscilloscope had good memory capacity allowing longer signals to be captured. Averaging of 100 samples provided an effective method for improving the SNR and more averages could be used, although this would increase the time required to perform the measurements. In this measurement the use of a narrow frequency band signal is advantageous for exciting a single mode of propagation. The use of a narrow bandpass filter as a post-processing step to reduce noise was effective in this situation.

The USB oscilloscope had the advantages of lower cost and portability. At an estimated cost of USD 1110 it is believed that this would be accessible for most research and practical applications. The small size and portability of USB oscilloscopes would be an advantage over bench-

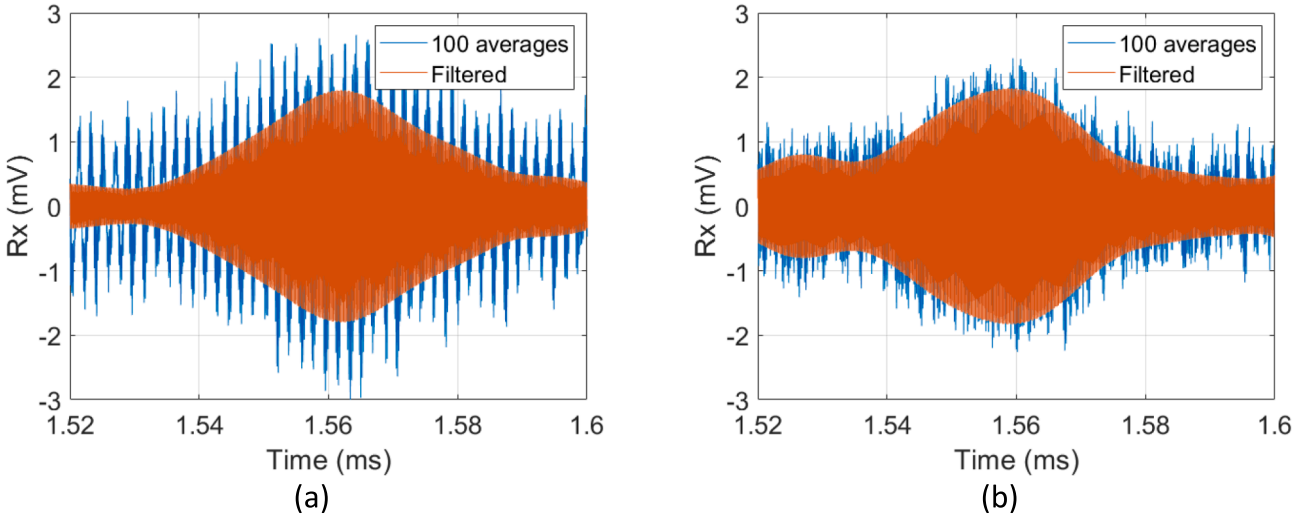


Fig. 9. Comparison of the two oscilloscopes for measuring the 5th arrival: (a) bench-top instruments (b) USB oscilloscope.

top instruments if experiments are to be performed in a mine. The small size and low cost of USB oscilloscopes may make these devices suitable for inclusion in commercial instruments for inspections of installed rock bolts. It is recommended that a pre-amplifier be used if the oscilloscope has a relatively high internal noise level. The use of a pre-amplifier with greater gain could be investigated in future. Longer range detection would be aided by increasing the excitation voltage applied to the transmit transducer, using a more powerful amplifier. Powerful amplifiers are available in expensive research equipment, and it is expected that if this equipment was used the drive signal could be increased by a factor of ten providing an additional 20 dB of SNR, which would allow one more reflection to be detected. Additional electronics to allow pulse-echo measurements, using a single transducer, could be investigated in the future. This could be achieved by including passive expander and limiter diode circuits or active switches in the measurement electronics, requiring a trade-off between performance and complexity. This would enable measurements to be performed on installed rock bolts where only one end is exposed. The developed low-cost measurement setup could be used to perform experiments on the propagation, attenuation, scattering, and transduction in rock bolts and other waveguides in the laboratory to quantify the influence of actual application conditions before attempting inspections in a mine. This could include installation of the rock bolt in a concrete block with full or partial grouting using concrete or epoxy grouts and investigating the influence of the end of the rock bolt being cut at an angle. The required preparation of the exposed end of the rock bolt and attachment of the transducer could be investigated in the laboratory. The likelihood of achieving successful inspections in a mine would be improved by addressing these and other practical constraints in the laboratory. Packaging of the instrumentation and compliance with mine safety requirements would be required before measurements can be conducted on rock bolts in mines.

CRediT authorship contribution statement

Philip W. Loveday: Writing – review & editing, Writing – original draft, Methodology, Investigation, Funding acquisition, Conceptualization. **Paul Fromme:** Writing – review & editing, Writing – original draft, Methodology, Investigation, Funding acquisition.

Declaration of competing interest

The authors declare that they have no known competing financial interests or personal relationships that could have appeared to influence the work reported in this paper.

Data availability

Data will be made available on request.

Acknowledgements

The authors gratefully acknowledge the financial support received from the UCL-Wits Strategic Partnership Fund.

References

[1] Olisa SC, Khan MA, Starr A. Review of current guided wave ultrasonic testing (GWUT) limitations and future directions. Sensors 2021;21(3):811. https://doi.org/10.3390/s21030811.
[2] Rose J, Avioli M, Song W. Application and potential of guided wave rail inspection. Insight 2002;44(6):353–8.
[3] Loveday PW. Guided wave inspection and monitoring of railway track. J Nondestr Eval 2012;31(4):303–9. https://doi.org/10.1007/s10921-012-0145-9.
[4] Legg M, Yücel MK, Kappatos V, Selcuk C, Gan T-H. Increased range of ultrasonic guided wave testing of overhead transmission line cables using dispersion compensation. Ultrasonics 2015;62:35–45. https://doi.org/10.1016/j.ultras.2015.04.009.
[5] Cawley P. A development strategy for structural health monitoring applications. J Nondestruct Eval Diagn Progn Eng Syst 2021;4. https://doi.org/10.1115/1.4051974.
[6] Beard MD, Lowe MJS. Non-destructive testing of rock bolts using guided ultrasonic waves. Int J Rock Mech Min Sci 2003;40(4):527–36. https://doi.org/10.1016/S1365-1609(03)00027-3.
[7] Lowe MJS, Alleyne DN, Cawley P. Defect detection in pipes using guided waves. Ultrasonics 1998;36(1–5):147–54. https://doi.org/10.1016/S0041-624X(97)00038-3.
[8] Rose JL. In: Ultrasonic guided waves in solid media. Cambridge: Cambridge University Press; 2014. https://doi.org/10.1017/CBO9781107273610.
[9] Zang X, Xu Z-D, Lu H, Zhu C, Zhang Z. Ultrasonic guided wave techniques and applications in pipeline defect detection: a review. Int J Press Vessel Pip 2023;206:105033. https://doi.org/10.1016/j.ijpvp.2023.105033.
[10] Bačić M, Gavin K, Kovačević MS. Trends in non-destructive testing of rock bolts. J Croat Assoc Civ Eng 2019;71(10):823–31. https://doi.org/10.14256/JCE.2727.2019.
[11] Bombarda D, Vitetta GM, Ferrante G. Rail diagnostics based on ultrasonic guided waves: an overview. Appl Sci 2021;11(3):1–42. https://doi.org/10.3390/app11031071.
[12] Masmoudi M, Yaacoubi S, Koabaz M, Akrout M, Skaiky A. On the use of ultrasonic guided waves for the health monitoring of rails. Proc Inst Mech Eng, Part F: J Rail Rapid Transit 2022;236(5):469–89. https://doi.org/10.1177/09544097211025898.
[13] Dalton RP, Cawley P, Lowe MJS. The potential of guided waves for monitoring large areas of metallic aircraft fuselage structure. J Nondestr Eval 2001;20(1):29–46. https://doi.org/10.1023/A:1010601829968.
[14] Leckey CAC, Rogge MD, Raymond Parker F. Guided waves in anisotropic and quasi-isotropic aerospace composites: three-dimensional simulation and

experiment. Ultrasonics 2014;54(1):385–94. https://doi.org/10.1016/j.ultras.2013.05.007.
[15] P. Fromme, "Guided Wave Testing," in *Handbook of Advanced Non-Destructive Evaluation*, N. Ida and N. Meyendorf, Eds., Cham: Springer International Publishing, 2018, pp. 1–30. 10.1007/978-3-319-30050-4_24-1.
[16] B. Pavlakovic, M. Lowe, D. Alleyne, P. Cawley. "Disperse: A General Purpose Program for Creating Dispersion Curves," in *Review of Progress in Quantitative Nondestructive Evaluation: Volume 16A*, D. O. Thompson and D. E. Chimenti, Eds., Boston, MA: Springer US, 1997, pp. 185–192. 10.1007/978-1-4615-5947-4_24.
[17] Loveday PW, Long CS, Ramatlo DA. Ultrasonic guided wave monitoring of an operational rail track. Struct Health Monit 2020;19(6). https://doi.org/10.1177/1475921719893887.
[18] Peter K, et al. An overview of the use of rockbolts as support tools in mining operations. Geotech Geol Eng 2022;40(4):1637–61. https://doi.org/10.1007/s10706-021-02005-5.
[19] Maepa TG, Zvarivadza T. Installation of resin-grouted rockbolts in hard rock mining: challenges and solutions for improved safety. J South Afr Inst Min Metall 2017;117(4):329–36. https://doi.org/10.17159/2411-9717/2017/v117n4a3.
[20] Villaescusa E, Varden R, Hassell R. Quantifying the performance of resin anchored rock bolts in the Australian underground hard rock mining industry. Int J Rock Mech Min Sci 2008;45(1):94–102. https://doi.org/10.1016/j.ijrmms.2007.03.004.
[21] M.D. Beard, *Guided Wave Inspection of Embedded Cylindrical Structures*, no. January. PhD Thesis, Imperial College, 2002.
[22] Buys BJ, Heyns PS, Loveday PW. Rock bolt condition monitoring using ultrasonic guided waves. J South Afr Inst Min Metall 2009;109(2):95–105.
[23] T. Stepinski, K.J. Mattson. "Instrument for rock bolt inspection by means of ultrasound," in *2015 IEEE International Ultrasonics Symposium, IUS 2015*, Institute of Electrical and Electronics Engineers Inc., 2015. 10.1109/ULTSYM.2015.0343.
[24] Zima B, Rucka M. Non-destructive inspection of ground anchors using guided wave propagation. Int J Rock Mech Min Sci 2017;94:90–102. https://doi.org/10.1016/j.ijrmms.2017.03.005.
[25] Stepinski T. Novel instrument for inspecting rock bolt integrity using ultrasonic guided waves. Measurement 2021;177. https://doi.org/10.1016/j.measurement.2021.109271.
[26] P. Loveday. "High frequency guided wave ultrasound measurements using low-cost equipment," in *12th South African Conference on Computational and Applied Mechanics, SACAM 2020*, EDP Sciences, 2020. 10.1051/matecconf/202134700010.
[27] Sun H, Zhu J. Nondestructive evaluation of steel-concrete composite structure using high-frequency ultrasonic guided wave. Ultrasonics 2020;103. https://doi.org/10.1016/j.ultras.2020.106096.
[28] Seco F, Jiménez AR. In: Modelling the Generation and Propagation of Ultrasonic Signals in Cylindrical Waveguides. Rijeka: IntechOpen; 2012. p. 1. https://doi.org/10.5772/29804.
[29] B. Pavlakovic, M. Lowe. "A General Purpose Approach to Calculating the Longitudinal and Flexural Modes of Multi-Layered, Embedded, Transversely Isotropic Cylinders," in *Review of Progress in Quantitative Nondestructive Evaluation: Volume 18A–18B*, D. O. Thompson and D. E. Chimenti, Eds., Boston, MA: Springer US, 1999, pp. 239–246. 10.1007/978-1-4615-4791-4_29.
[30] G. Petersen. "L-Matching the Output of a RITEC Gated Amplifier to an Arbitrary Load," *RITEC Inc., USA, www.RitecInc.com.* 2006. [Online]. Available: www.RitecInc.com.